Eur Radiol (2008) 18: 2731–2738
DOI 10.1007/s00330-008-1089-4



**Tobias Achenbach**
**Oliver Weinheimer**
**Alexander Biedermann**
**Sabine Schmitt**
**Daniela Freudenstein**
**Edula Goutham**
**Richard Peter Kunz**
**Roland Buhl**
**Christoph Dueber**
**Claus Peter Heussel**

# MDCT assessment of airway wall thickness in COPD patients using a new method: correlations with pulmonary function tests

Received: 15 October 2007
Revised: 12 May 2008
Accepted: 24 May 2008
Published online: 19 July 2008


T. Achenbach (✉) · O. Weinheimer · S. Schmitt · D. Freudenstein · R. P. Kunz · C. Dueber
Department of Diagnostic and Interventional Radiology, Johannes Gutenberg University, Langenbeckstrasse 1, 55101 Mainz, Germany
e-mail: achenbac@uni-mainz.de
Tel.: +49-6131-177358
Fax: +49-6131-173413

A. Biedermann · R. Buhl
IIIrd Department of Internal Medicine - Pneumology, Johannes Gutenberg University, Langenbeckstraße 1, 55101 Mainz, Germany

E. Goutham
Astra Zeneca, Lund, Sweden

C. P. Heussel
Diagnostic and Interventional Radiology, Thoraxklinik, University Hospital Heidelberg, 69126 Heidelberg, Germany

**Abstract** Quantitative assessment of airway-wall dimensions by computed tomography (CT) has proven to be a marker of airway-wall remodelling in chronic obstructive pulmonary disease (COPD) patients. The objective was to correlate the wall thickness of large and small airways with functional parameters of airflow obstruction in COPD patients on multi-detector (MD) CT images using a new quantification procedure from a three-dimensional (3D) approach of the bronchial tree. In 31 patients (smokers/COPD, non-smokers/controls), we quantitatively assessed contiguous MDCT cross-sections reconstructed orthogonally along the airway axis, taking the point-spread function into account to circumvent over-estimation. Wall thickness and wall percentage were measured and the per-patient mean/median correlated with FEV1 and FEV1%. A median of 619 orthogonal airway locations was assessed per patient. Mean wall percentage/mean wall thickness/median wall thickness in non-smokers (29.6%/0.69 mm/0.37 mm) was significantly different from the COPD group (38.9%/0.83 mm/0.54 mm). Correlation coefficients ($r$) between FEV1 or FEV1% predicted and intra-individual means of the wall percentage were −0.569 and −0.560, respectively, with $p<0.001$. Depending on the parameter, they were increased for airways of 4 mm and smaller in total diameter, being −0.621 (FEV1) and −0.537 (FEV1%) with $p<0.002$. The wall thickness was significantly higher in smokers than in non-smokers. In COPD patients, the wall thickness measured as a mean for a given patient correlated with the values of FEV1 and FEV1% predicted. Correlation with FEV1 was higher when only small airways were considered

**Keywords** Airway obstruction · Chronic obstructive pulmonary disease · Helical computed tomography · Computer-assisted diagnosis

## Introduction

Bronchial wall thickening is a well described post-mortem sign of chronic obstructive bronchitis, which is frequently assosciated with chronic obstructive pulmonary disease (COPD) [1]. The possibility to depict the airway wall by computed tomography (CT) or endobronchial ultrasound (EBUS) has confirmed these findings and CT has become the "gold standard" for airway imaging due to its minimal invasiveness and as a result of the development of multi-detector CT (MDCT). MDCT helps to assess the phenotype of COPD as patients with predominantly emphysematous

disease may not show signs of airway inflammation [2–6]. Recently, published studies have provided clearer details about the architecture and histopathological changes in the airway wall. Nearly all layers of the airway wall, including epithelium, basement membrane, inner airway wall, smooth muscle layer, cartilage, outer wall, and adherent parenchyma, may be thickened; however, MDCT cannot distinguish these layers. Other changes, such as increased numbers of goblet cells or intraluminal mucus plugs, also cause thickening of the airway wall in MDCT [7–10]. One of the most detailed histopathological studies was published by Hogg and co-workers, who demonstrated that COPD progression is strongly associated with an increase in the volume of tissue in the wall and also with the accumulation of inflammatory mucus exudates in the lumen of airways less than 2 mm in diameter [10].

Although CT is not yet able to distinguish between the aforementioned layers, a relationship between CT-derived bronchial parameters and COPD severity is suspected and different studies have found evidence of a moderate correlation with functional parameters such as the forced expiratory volume in 1 s (FEV1) [4, 5, 11]. Additionally, a correlation between the wall thickness of airways visible on CT and smaller airways (internal diameter approximately 1.27 mm) that can only be measured by histological methods has been proven [12]. Thus, MDCT represents a potential scientific tool for quantifying inflammatory airway changes as a surrogate of airway wall remodelling in the small airways. According to our research findings from the last 5 years, morphometry of the airway walls can deliver grossly false results, especially in smaller airways and particularly if automated techniques such as the full-width-at-half-maximum principle (FWHM) are applied that do not take into account the point-spread function inherent to all MDCT systems [13, 14]. The wall of more distal airways can easily be over-estimated, thus erroneously indicating a relative thickening compared with the more central airways and leading to the questionable conclusion that the increase in FEV1 in COPD patients is determined by the more peripheral airway wall properties and not the more central ones [11]. The aim of this work was to investigate whether the results of those studies were skewed by the point-spread effect.

Furthermore, we wanted to test the feasibility of the airway analysis module we developed as a part of a software called YACTA ("yet another CT analyser"), which is described further in the "Materials and methods" section.

## Materials and methods

### Patients and imaging

A total of 40 patients examined using thin-section MDCT of the chest for different clinical reasons (35 malignancies, one suspicion of pulmonary embolism, four COPD assessments) were included prospectively into this study, which was approved by an institutional review board. Each patient gave informed consent. Two study groups ($n$=20 each) were established, recruiting never-smokers without any clinical symptoms of lung disease and smokers with COPD that had no exacerbation within the previous 6 weeks according to the GOLD criteria. After excluding nine individuals (five never-smokers, four smokers) with minimally differing CT parameters, we entered ten women and 21 men into the study. The 15 non-smokers were classified as GOLD stage 0, while the 16 smokers were staged as class 2 and 3 ($n$=8 each). Stages 1 and 4 were not observed during recruitment. Further demographic data are shown in Table 1.

CT examinations included in the study were carried out at full inspiration with a Siemens VolumeZoom Plus 4, tube current 120 kV, 100 mAs, rotation time 0.5 s, pitch 0.8 (table feed 4 mm per rotation); collimation was 4× 1.25 mm. Reconstruction increment was 1 mm and a reconstruction kernel of b40f was used additionally with a field of view (FOV) adapted to the patient's lung. A second FOV of 200 mm was centered on the bronchial tree. The resulting voxel size was 0.391×0.391×1.25 mm. A mean number of 300 images was acquired, giving an average effective dose of 5.7 mSv (female) and 4.4 mSv (male) per patient.

**Table 1** Clinical data of all study patients (*SD* standard deviation)

| | Smoker | | Never-smoker | |
|---|---|---|---|---|
| | Mean ± SD | Range | Mean ± SD | Range |
| Gender (male/female) | 16/4 | | 11/9 | |
| Age (years) | 65±7 | 50–75 | 65±14 | 34–85 |
| Smoking index (pack years) | 52±25 | 21–135 | 0 | 0 |
| Height (cm) | 170±0 | 148–189 | 171±0 | 148–186 |
| Weight (kg) | 74±20 | 54–119 | 84±27 | 59–180 |
| Body mass index | 25±6 | 19–38 | 29±9 | 20–60 |
| FEV1 (l/s) | 1.55±0.6 | 0.71–2.81 | 2.9±0.7 | 1.33–3.95 |

The lung function tests were performed within a median time interval of 8 days (mean 12.3 days, minimum 0 days, maximum 76 days) after the CT according to the recommendations of the European Respiratory Society (ERS). Short-acting β2-agonists were withheld for 8 h and long-acting β2-agonists, inhaled anticholinergics, xanthine derivatives, and antihistamines for 24 h before testing. A flow plethysmograph (Jaeger Masterlab Spirometer, Jaeger, Würzburg, Germany) was used for the examination. For each subject, the largest FEV1, the forced vital capacity (FVC), and the vital capacity (VC) out of a minimum of three and a maximum of eight were selected.

## Computer-aided evaluation - YACTA

YACTA is the preliminary name of a custom-made software tool programmed in C++ (O.W.). Its modular capabilities in lung segmentation and emphysema detection and quantification have been described previously [15, 16]. Airway segmentation was already part of the emphysema tool developed to prevent misclassifying airways as emphysematous lung parenchyma. This standard technique is performed on the basis of region-growing algorithms and details about the procedure are reported in the aforementioned study. As we aim to assess airway parameters in the bronchi in the transverse and oblique planes, a skeletonization of the bronchial tree is added. A topology-preserving, three-dimensional (3D) thinning algorithm is used, resulting in a skeleton-like view of the bronchial tree, similar to the procedure of Palagyi et al. [17]. The voxel-based results of the skeletonization are rendered graphically, similar to the method of Tschirren et al. [18]. A slice orthogonal to the skeleton axis can be shown and interactively moved through the airways by calculating the orientation of the airway using the graph and skeleton information. Within this slice, the measurements are carried out. Thus, the radiologist can assess the morphometric parameters of bronchi orthogonally (2D mode) and the parameters of airways crossing the image plane obliquely (Fig. 1). In case of attendant vessels, the adjacent wall parts or even the entire slice is not used for wall assessment, depending on the generated grey level profile (see below). The parameters measured directly include: lumen voxel count (number) and surface ($mm^2$), total diameter (mm), luminal and wall area ($mm^2$), mean wall thickness (mm), and median wall thickness (mm) (after excluding the extremes per reconstructed slice). The parameters calculated with the help of the measured parameters were: lumen area from voxel count ($mm^2$), calculated lumen area ($mm^2$), wall area ($mm^2$), wall percentage (percent share of the whole bronchus cross-sectional area), airway generation number, and angle between airway and axial slice.

Basic elements of each measurement are virtual rays sent out centrifugally from a centre point of the airways. A similar method called “ray casting” has already been described by Amirav et al. [19, 20], but those results are transferred to a completely 3D method. Grey-level profiles are detected along each respective ray’s path. The estimation of the airway wall border is hampered by the spread-point function of all CT scanners: CT over-estimates the size of small objects and under-estimates the density [21]. The use of assessment techniques, FWHM in particular, can over-estimate the airway wall thickness. Figure 2 illustrates the dilemma in estimating airway-wall thickness. To overcome this problem we used the previously established integral-based method (IBM) [13]. This formula reverses the effects of the scanner’s point-spread function insofar as we have observed in our phantom studies on plastic tubes. Therefore, the integral under the profile is kept constant, while the profile itself is transformed, narrowed, and elevated. To apply this method, knowledge of the tissue density is mandatory. From our phantom studies we estimated that 50 HU reflects the bronchial densities most adequately.

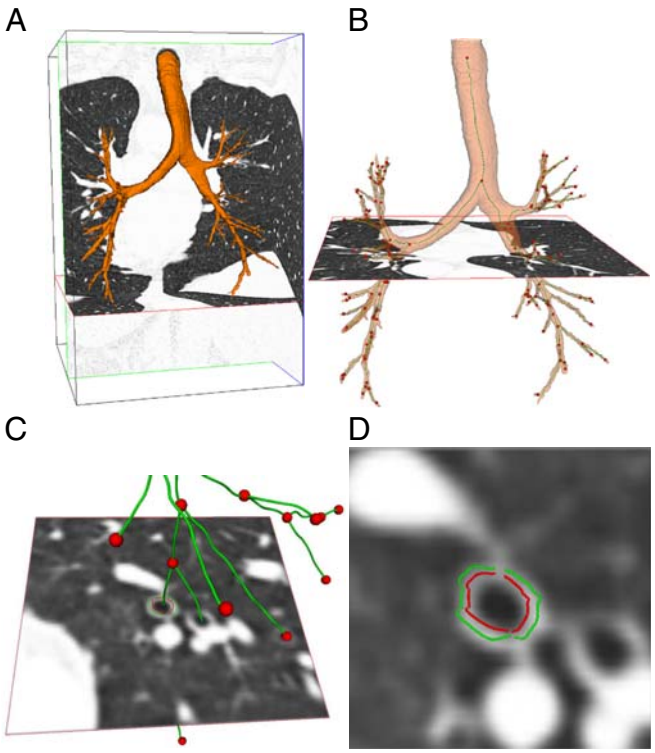


**Fig. 1** **a** Coloured overlay of the airway segmentation result within a part of the whole voxel cube of the MDCT data set. **b** Result of the following skeletonization and an axial slice on the level of the bronchus intermedius. **c** Reconstructed slice orthogonal to the resulting axis (*green*) of the centrally depicted bronchus at the subsegmental level. The *small red spheres* represent branching points of the airway skeleton. **d** Orthogonal slice with a coloured overlay showing the detected edges of the internal (*red*) and external (*green*) bronchial wall assessed on the basis of the ray-casting method with its centre on the green central axis. In some parts YACTA does not accept the grey level profile of the ray that has been cast (e.g. in the 12 o’clock position). For further calculation, extremes and outliers are also eliminated

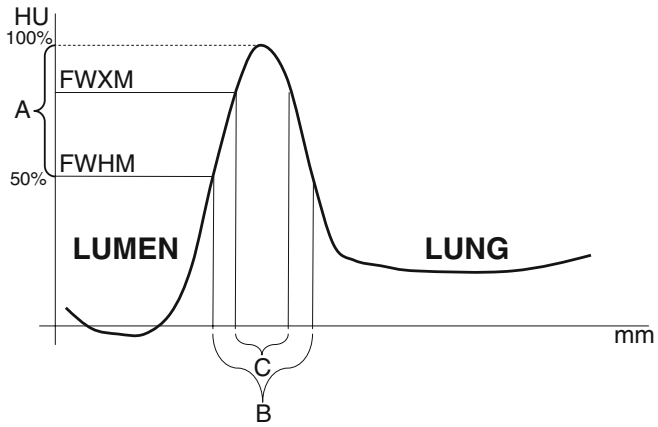


**Fig. 2** Shows a model of a grey-level profile of a ray along its way across the bronchial wall. When using the FWHM principle, the beginning and the end of the bronchial wall are assumed at the 50% level (*vertical line* at 50%) related to the profile's apex (*dashed line* at 100%). Airway wall thickness would be demonstrated by *bracket B*. The FWHM method showed incorrect results in airway walls smaller than 1.5–1.0 mm in our phantom studies. The *vertical bracket* shows the range, where the real borders of the airway wall would be expected. The corresponding thickness must be smaller than *B*, for example, at the level of FWXM (full width at X percentage of maximum, *bracket C*)

### Post-processing and statistics

All CT data sets were analysed using YACTA as described above. The segmentation results were controlled visually. The morphometric airway parameters employed included: total airway diameter, wall percentage, mean wall thickness, and median wall thickness. Statistical analysis was performed with SPSS 11. Descriptive statistics and comparison of means of the wall percentage and FEV1 were analysed by using Mann-Whitney's *U*-test, similar to the method of Hasegawa et al. [11]. Following this study, we analysed all measurable airways and additionally analysed smaller bronchi as a separate entity. Although there is no clear nomenclature, an inner diameter of about 2.3 mm (±0.6) and a wall thickness about 0.9 mm (±0.2) were attributed to bronchi of the sixth generation size in the aforementioned study. This corresponds to bronchi with a total diameter of 4 mm and below in our data. This subgroup was correlated with FEV1 in the same way. Additionally, we set up graphic correlations of FEV1 and the wall percentage as described in [11] and added intra-individual empirical observations from the scatter diagrams of all patients, including all the YACTA measurements between the total airway diameter (mm) and the wall percentage (%).

## Results

Altogether, 18,628 bronchial, orthogonal slices were analysed successfully (maximum per patient 1,070, minimum per patient 212; median 619, mean 601). Empirical analysis showed that YACTA achieved most measurements in longer bronchi, which were found more frequently at the subsegmental level. Short bronchi, where a higher percentage consisted of an airway crossing, provided only few or no usable data because YACTA automatically detected and excluded locations where the airway wall was not representative for the whole segment (e.g., bifurcations, trifurcations). A mean of 7.9 slices could be measured per segmented bronchus (standard deviation 6.99, range 50). In the central regions of the trachea and the main bronchi, measurements were complicated by surrounding soft tissue and fewer locations could be analysed than at the subsegmental level. The airways were labelled in generations, which was frequently incorrect; for example, if YACTA missed a small bronchus branching out (these locations were automatically excluded from further assessment) or if YACTA added nonanatomical branching points in larger airways. Bronchial analysis was not affected by these misclassifications and generation numbers were not used for further analysis. Descriptive data are given in Table 2.

The non-parametric Mann-Whitney's *U*-test showed significant differences ($p<0.001$) in the wall percentage and the wall thickness between never-smokers and smokers (GOLD stages 2 and 3) (Fig. 3). There was no significant difference between a GOLD stage 2 and GOLD stage 3 group concerning mean wall percentage and mean wall thickness ($p_{\text{wall percentage}}=0.294$, $p_{\text{wall-thickness}}=0.753$). The correlation between FEV1 [FEV1% (FEV1 percent of predicted normal)] and the wall percentage was $r=-0.569$ ($r=-0.560$) for all analysed airways, whereas correlation between FEV1

**Table 2** YACTA's results of the total diameter, the wall percentage, the mean wall thickness and the median wall thickness of all analysed airways

| | Never smokers | | Smokers (GOLD 2 and 3) | |
|---|---|---|---|---|
| | Mean ± SD | Range | Mean ± SD | Range |
| Total diameter (mm) | 4.5±0.2448 | 4.1–5.0 | 4.7±0.341 | 4.3–5.8 |
| Wall percentage (%) | 29.6±4.093 | 24.7–40.5 | 38.9±7.421 | 25.4–51.7 |
| Mean wall thickness (mm) | 0.69±0.0716 | 0.57–0.85 | 0.83±0.145 | 0.63–1.17 |
| Median wall thickness (mm) | 0.37±0.0538 | 0.31–0.53 | 0.54±0.12 | 0.36–0.79 |

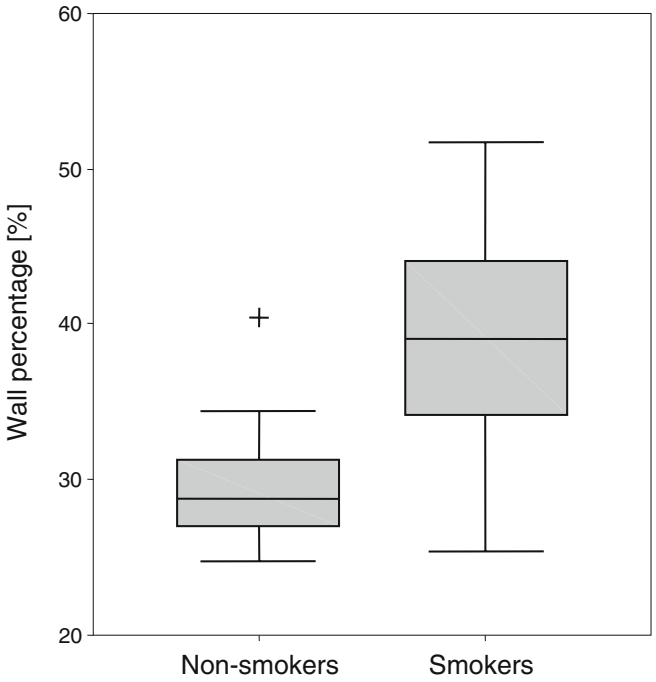


**Fig. 3** Boxplot diagram of the mean wall percentage categorized by the smoking status. *Horizontal lines within the grey standard deviation boxes* represent the median wall percentage of its group. *Thin black lines* represent the extreme numbers (range), + represents a single outlier (1.5-times beyond the standard deviation box). Difference was significant ($p<0.001$; Mann-Whitney's *U*-test)

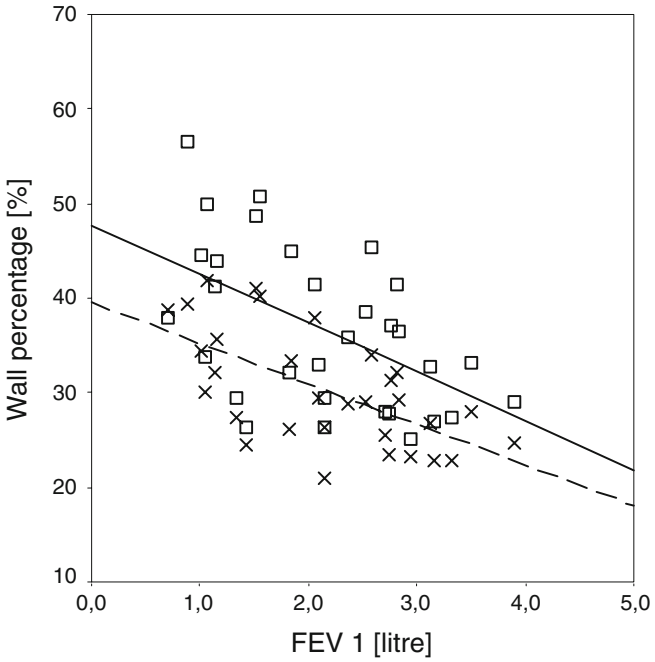


**Fig. 4** Overlay scatter diagram illustrates the minor distinction of the wall percentage of airways with a total diameter greater than 4 mm and bronchi with a total diameter of 4 mm and smaller of all patients. Note the lower scatter cloud compared with other studies, indicating the reduced risk of potential overestimation of the airway wall thickness caused by the scanner's spread point function. Linear regression lines: *open squares and continuous line* airways with total diameters greater than 4 mm ; *crosses and dashed line* airways with total diameters smaller or equal 4 mm

(FEV1%) and the wall percentage for airways of 4 mm diameter in total and smaller was $r=-0.621$ ($r=-0.537$) and for airways greater than 4 mm in diameter $r=-0.532$ ($r=-0.541$). Detailed results and correlation coefficients ($r$) are also given in Table 3.

To demonstrate the difference between the proximal and the more distal airways, the relationship between FEV1 and the wall percentage was plotted in a scatter correlation diagram (Fig. 4). The diagram showed a very homogeneous scattering of the different airway entities with a subjectively slight shift of the scatter cloud of all airways to the higher wall percentages. The range of wall percentage was 25.6–52.7%.

Empirical analysis of the scatter correlation graphics of all patients showed that on these diagrams morphology for the two individuals with the highest and lowest FEV1% (extremes) of all patients was different (Fig. 5). The patient with the lowest FEV1% showed a flat fitting curve created by quadratic regression and a very concentrated scatter cloud. The wall percentages closely approached the 70% level and the scatter cloud was spread along the *x*- and the *y*-axis. The diagram of the patient with the highest FEV1% was 91% and showed a steeper fitting line and the highest wall percentages did not reach the 60% level. Although the

**Table 3** Pearson's correlation coefficients of FEV1 and means of wall percentage and median wall thickness. Results are ordered by airway size. Significance is marked: coefficients in *bold* have $p<0.001$; coefficients in *italics* have $p<0.002$. A tendency for higher correlation of functional parameters and morphometric numbers at the more distal airways can be seen for the wall percentage and the median wall thickness for the FEV1, but not for the FEV1% predicted. Notice that the coefficients of significance are all arrayed within a similar level

| | Correlation coefficient *r* between FEV1 or FEV1% predicted and: | | | | | |
|---|---|---|---|---|---|---|
| | Wall percentage (%) | | Median wall thickness (mm) | | Mean wall thickness (mm) | |
| | FEV1 | FEV1 (% predicted) | FEV1 | FEV1 (% predicted) | FEV1 | FEV1 (% predicted) |
| All airways | **−0.569** | **−0.560** | **−0.577** | **−0.620** | **−0.587** | **−0.561** |
| Airways > 4 mm | *−0.532* | *−0.541* | **−0.552** | **−0.616** | **−0.580** | **−0.568** |
| Airways ≤4 mm | **−0.621** | *−0.537* | **−0.628** | **−0.546** | **−0.548** | −0.423 |

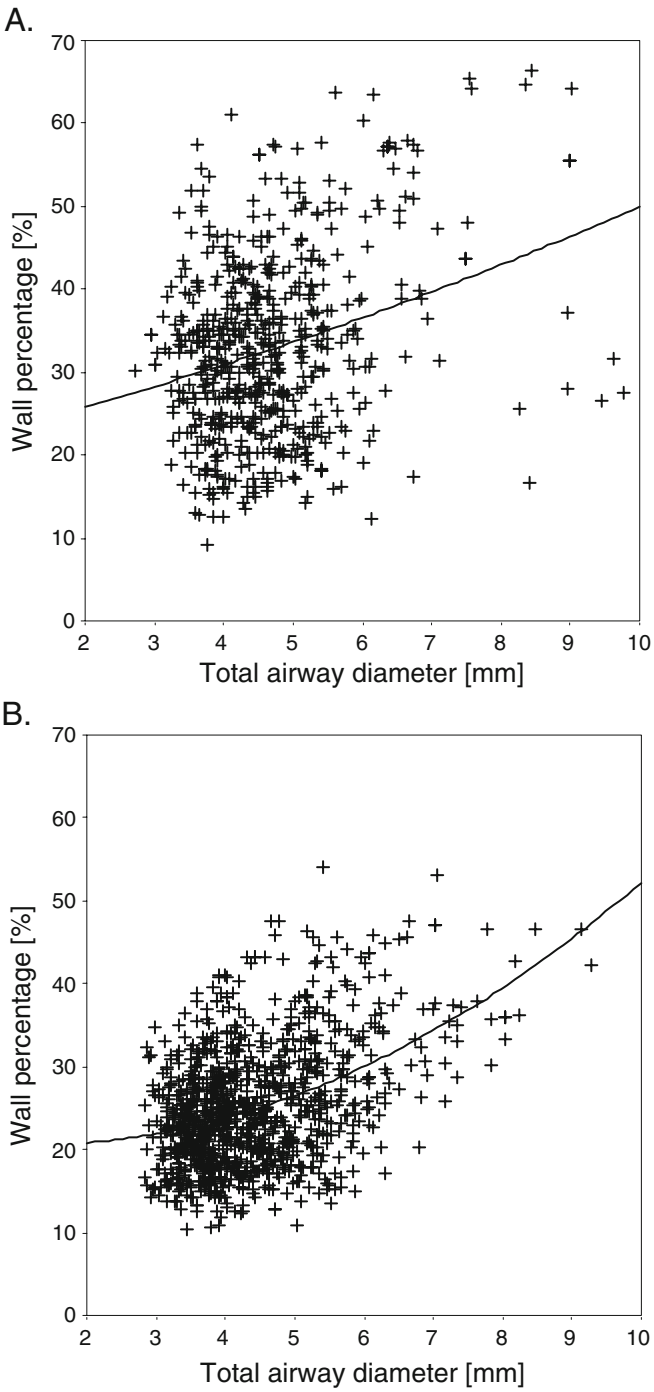


**Fig. 5** **a** Scatter correlation diagram of the total airway diameter and the wall percentage of the COPD patient with the lowest FEV1%. All YACTA measurements of this one patient are included. The *black line* is the fitted line obtained by quadratic regression. **b** The same graphic correlation of the non-COPD patient with the highest FEV1%. Note the elevated and spread scatter cloud of the functionally impaired patient showing higher wall percentages in comparable total airway diameters

FEV1 extremes differed clearly in their graphic appearance, this was not consistent with the FEV1 - extreme pairs closer to the median. In other words, individual smokers or never-smokers could not be distinguished by these diagrams.

## Discussion

We used a new software tool (YACTA) for airway morphometry in a limited, but sharply defined study population of patients suffering from COPD (smokers) and healthy never-smoker controls. The crucial point-spread function (PSF) distorts the image of very small objects, such as the airway wall, and this is inherent to every CT system [21]. Compensation for this effect within an orthogonally reconstructed airway slice was implemented for the first time using a new, integral-based method, which proved to be highly accurate and reproducible in anthropomorphic phantom studies and porcine CT images [13]. According to several earlier studies using different techniques, YACTA found significant differences between the wall percentages of the two patient groups [22, 23]. Thus, function and feasibility have been demonstrated.

The aim of our study was to correlate morphology and function. An artificial increase in more distal bronchial wall thickness due to the PSF could potentially cause a falsely increased correlation between FEV1 and wall percentage in smaller airways than in larger airways. Furthermore, we wanted to verify the current literature. Therefore, the decision to look separately at bronchi characterised by a total diameter that is equal to or smaller than 4 mm was oriented toward the procedure used by other study groups and is of course arbitrary and open to debate. Pathologic studies have reported differing sites of structural airway changes in COPD, but airways with a (microscopically assessed) diameter of less than 2 mm are repeatedly involved [24]. In our patient group we detected bronchi with minimal diameters of 2.7 mm, which is a very good result for a MDCT study but is still beyond the histological definition of “small airways”, especially as only few of those small bronchi could be segmented. Therefore, like other study groups, we geared our border between “more central” and “more distal” airways, according to previous publications [4, 5, 11]. In our data, the bronchi of the sixth generation (used as a landmark by Hasegawa et al. [11]) had a total wall thickness of about 1 mm and smaller, thus justifying this selection to gain comparable results. In other words: according to Hasegawa and co-workers, sixth generation bronchi had a total diameter of approximately 4 mm. The higher correlation between function and distal airways was observed in our analysis, too. We found moderate but significant correlations with $r=-0.569$ for all airways, $r=-0.532$ for airways larger than 4 mm, and $r=-0.621$ for bronchi of 4 mm in total diameter and smaller. Thus, on the one hand, the hypothesis that FEV1 can be

determined within the peripheral airways seems to be proven but, on the other hand, this bears no significance for relative FEV %. However, our study could not establish whether this lack of significance was due to the compensation of the PSF or the low expression of the relative FEV1 in patients with higher grades of obstruction. Because of this possible effect, we prefer to indicate both relative and absolute FEV1, while other studies use only the relative FEV1 [11]. However, our correlation coefficients exceed or partly match the levels of other studies that reported correlations of $r$=0.04-0.55, confirming that function and CT findings are connected to each other. Earlier studies showed a connection between function and emphysema amount, too, but the present study focused on airway remodelling.

Several drawbacks of our study should be mentioned. First of all and as in other studies, our technique was not radiologically-pathologically calibrated or correlated. Post mortem inconsistencies between lung parenchyma and airways represent a major problem that has not yet been resolved. In particular, changes in airway size and morphology would represent fundamental incomparability. Other studies have tried to quantify airway walls, e.g. via manual dilatation of a digital microscope image of the bronchus deformed by microtome cutting, which introduced a very high variability [10]. To our knowledge, only two study groups have compared CT parameters with pathological specimens (sheep and humans). One of them analysed the mechanical properties and not the CT assessment of bronchi but rather semi-automatically measured density in inspiratory and expiratory scans [22]. This group used a fixation technique with formalin steam introduced by Weibel in 1961 [25–27]. The other group, using the FWHM principle, clearly identified an overestimation of the airway wall caused by the point-spread function but gave no solution for this problem [12]. Other groups worked with partly artificial phantoms in an isolated lung, where the quantified objects were made of wax and had a well-known size, which is not possible in an airway setting [28, 29]. Our phantom study worked with wall thicknesses comparable with distal airways, distinguishing it from other trials. We expect that the relative errors derived from measurements in human beings are slightly higher as the parenchyma-bronchi border is surely less sharp. However, even interpolating the relative error for in vivo measurement to 20% accuracy has to be considered as high, especially when compared with standard study results [30].

Secondly, the resolution was slightly inferior to current MDCT technology. Slice thickness was 1.25 mm; however, newer scanners could achieve a slice thickness of about 0.8 mm. This must be mentioned as resolution is a crucial point here. On the other hand, we subsequently decreased the FOV and increased the in-plane resolution, which is an advantage for the resolution of the relevant orthogonal slices compared with other studies.

Thirdly, airway labelling capabilities were limited: small bronchi branching off were missed, which was not quantified any further as a high variability hampers correct designation of the airways [31]. This had no effect on further assessment of the airway wall thickness, though, as the ray-casting algorithm automatically excluded those locations from the assessment. However, we refrained from further evaluation related to airway generation in order to avoid errors.

Finally, we did not analyse our patients with the FWHM technique, which could have brought further insight into the influence of over-estimation on the correlation.

On the other hand, important advantages of our study should be mentioned: a high amount of cross-sectional airway locations were analysed per patient. Other studies are often limited to bronchi depicted cross-sectionally. In particular, the origin of the right apical bronchus is frequently chosen because of its specific orientation to the image plane. Nakano et al. [4] correlated the results of measuring this particular bronchus with 20 additionally assessed bronchi measurements and found a high correlation, thus justifying their selection. However, this technique still represents a limitation if focal airway changes are expected similar to various other studies [25, 26, 32]. Our technique overcomes this limitation. Other methods search for nearly cross-sectionally depicted bronchi [30]. In our understanding of diffuse airway disease assessment of as many locations as possible is important in order to understand where certain pathological conditions occur. Only a few studies give hints about this and demonstrate that, for example, airflow limitation in COPD is more closely related to the dimension of the distal (smaller) airways than to the proximal (larger) airways [11]. On the other hand, there is no commonly accepted definition of central or peripheral or small or large airways. Hasegawa and co-workers use the term “generation”. Measuring the third to the sixth generation right apical bronchus (B1) and the right anterior basal bronchus, they found wall thicknesses from 1.3 to 0.9 mm. Their study is restricted to two bronchi, which could serve as a source of bias. In our study, as many measurements as technically possible were used, achieving a nearly complete assessment with up to 1,070 locations per patient, which has not been described previously. Therefore, influences of focal airway changes are assumed to be minimised.

The intra-individual graphic correlation of the wall percentage and the total airway diameter was an interesting exercise and the differences between the two diagrams of the patients with the two FEV1 extremes are quite impressive (Fig. 5). The great number of measured airway slices per patient made it possible to draw fitting lines calculated by quadratic regression on these scatter diagrams. This could be a future key for a more individual description of the airway status of a patient that would avoid the averaging used in this and other studies. These parameters could provide diagnostic hints beyond visual

accessibility of the source images. Finding focal airway pathologies simply by identifying outliers might represent another potential and even better clinical use of the YACTA technique and should be addressed in future studies.

## References


1. Gough J (1961) Post mortem differences in "asthma" and in chronic bronchitis. Acta Allergol 16:391–399
2. Huber HL, Koessler KK (1922) The pathology of bronchial asthma. Arch Intern Med 30:689–760
3. Grenier PA, Beigelman-Aubry C, Fetita C, Preteux F, Brauner MW, Lenoir S (2002) New frontiers in CT imaging of airway disease. Eur Radiol 12:1022–1044
4. Nakano Y, Muro S, Sakai H, Hirai T, Chin K, Tsukino M, Nishimura K, Itoh H, Pare PD, Hogg JC, Mishima M (2000) Computed tomographic measurements of airway dimensions and emphysema in smokers. Correlation with lung function. Am J Respir Crit Care Med 162:1102–1108
5. Orlandi I, Moroni C, Camiciottoli G, Bartolucci M, Pistolesi M, Villari N, Mascalchi M (2005) Chronic obstructive pulmonary disease: thin-section CT measurement of airway wall thickness and lung attenuation. Radiology 234:604–610
6. Aziz ZA, Wells AU, Desai SR, Ellis SM, Walker AE, MacDonald S, Hansell DM (2005) Functional impairment in emphysema: contribution of airway abnormalities and distribution of parenchymal disease. AJR Am J Roentgenol 185:1509–1515
7. Tiddens H, Silverman M, Bush A (2000) The role of inflammation in airway disease: remodeling. Am J Respir Crit Care Med 162:S7–S10
8. Haraguchi M, Shimura S, Shirato K (1996) Morphologic aspects of airways of patients with pulmonary emphysema followed by bronchial asthma-like attack. Am J Respir Crit Care Med 153:638–643
9. Hogg JC (2004) Pathophysiology of airflow limitation in chronic obstructive pulmonary disease. Lancet 364:709–721
10. Hogg JC, Chu F, Utokaparch S, Woods R, Elliott WM, Buzatu L, Cherniack RM, Rogers RM, Sciurba FC, Coxson HO, Pare PD (2004) The nature of small-airway obstruction in chronic obstructive pulmonary disease. N Engl J Med 350:2645–2653
11. Hasegawa M, Nasuhara Y, Onodera Y, Makita H, Nagai K, Fuke S, Ito Y, Betsuyaku T, Nishimura M (2006) Airflow limitation and airway dimensions in chronic obstructive pulmonary disease. Am J Respir Crit Care Med 173:1309–1315
12. Nakano Y, Wong JC, de Jong PA, Buzatu L, Nagao T, Coxson HO, Elliott WM, Hogg JC, Pare PD (2005) The prediction of small airway dimensions using computed tomography. Am J Respir Crit Care Med 171:142–146
13. Weinheimer O, Achenbach T, Bletz C, Düber C, Kauczor H-U, Heussel CP (2008) About objective 3-D analysis of airway geometry in computerized tomography. IEEE Trans Med Imag 27:64–74
14. Reinhardt JM, D'Souza ND, Hoffman EA (1997) Accurate measurement of intrathoracic airways. IEEE Trans Med Imag 16:820–827
15. Achenbach T, Weinheimer O, Buschsieweke C, Heussel CP, Thelen M, Kauczor HU (2004) Fully automatic detection and quantification of emphysema on thin section MD-CT of the chest by a new and dedicated software. Rofo 176:1409–1415
16. Heussel CP, Achenbach T, Buschsieweke C, Kuhnigk J, Weinheimer O, Hammer G, Duber C, Kauczor HU (2006) Quantification of pulmonary emphysema in multislice-CT using different software tools. Rofo 178:987–998
17. Palagyi K, Tschirren J, Sonka M (2003) Quantitative analysis of intrathoracic airway trees: methods and validation. Inf Process Med Imaging 18:222–233
18. Tschirren J, McLennan G, Palagyi K, Hoffman EA, Sonka M (2005) Matching and anatomical labeling of human airway tree. IEEE Trans Med Imag 24:1540–1547
19. Amirav I, Kramer SS, Grunstein MM (2001) Methacholine-induced temporal changes in airway geometry and lung density by CT. Chest 119:1878–1885
20. Amirav I, Kramer SS, Grunstein MM, Hoffman EA (1993) Assessment of methacholine-induced airway constriction by ultrafast high-resolution computed tomography. J Appl Physiol 75:2239–2250
21. Dougherty G, Newman D (1999) Measurement of thickness and density of thin structures by computed tomography: a simulation study. Med Phys 26:1341–1348
22. Berger P, Laurent F, Begueret H, Perot V, Rouiller R, Raherison C, Molimard M, Marthan R, Tunon-de-Lara JM (2003) Structure and function of small airways in smokers: relationship between air trapping at CT and airway inflammation. Radiology 228:85–94
23. Copley SJ, Wells AU, Muller NL, Rubens MB, Hollings NP, Cleverley JR, Milne DG, Hansell DM (2002) Thin-section CT in obstructive pulmonary disease: discriminatory value. Radiology 223:812–819
24. Jeffery PK (2001) Remodeling in asthma and chronic obstructive lung disease. Am J Respir Crit Care Med 164: S28–S38
25. Montaudon M, Berger P, de Dietrich G, Braquelaire A, Marthan R, Tunon-de-Lara JM, Laurent F (2007) Assessment of airways with three-dimensional quantitative thin-section CT: in vitro and in vivo validation. Radiology 242:563–572
26. Berger P, Perot V, Desbarats P, Tunon-de-Lara JM, Marthan R, Laurent F (2005) Airway wall thickness in cigarette smokers: quantitative thin-section CT assessment. Radiology 235:1055–1064
27. Weibel ER (1963) Morphometry of the human lung. Springer, Berlin New York
28. Bolte H, Muller-Hulsbeck S, Riedel C, Jahnke T, Inan N, Heller M, Biederer J (2004) Ex-vivo injection technique for implanting solid pulmonary nodules into porcine lungs for multi-slice CT. Rofo 176:1380–1384
29. Biederer J, Schoene A, Freitag S, Reuter M, Heller M (2003) Simulated pulmonary nodules implanted in a dedicated porcine chest phantom: sensitivity of MR imaging for detection. Radiology 227:475–483
30. Saba OI, Hoffman EA, Reinhardt JM (2003) Maximizing quantitative accuracy of lung airway lumen and wall measures obtained from X-ray CT imaging. J Appl Physiol 95:1063–1075
31. Ghaye B, Szapiro D, Fanchamps JM, Dondelinger RF (2001) Congenital bronchial abnormalities revisited. Radiographics 21:105–119
32. Awadh N, Muller NL, Park CS, Abboud RT, FitzGerald JM (1998) Airway wall thickness in patients with near fatal asthma and control groups: assessment with high resolution computed tomographic scanning. Thorax 53:248–253